optica

Realization of high-dimensional frequency crystals in electro-optic microcombs

YAOWEN HU,[1,2,†] CHRISTIAN REIMER,[1,3,†] AMIRHASSAN SHAMS-ANSARI,[1] MIAN ZHANG,[3] AND MARKO LONCAR[1,*]

[1]John A. Paulson School of Engineering and Applied Sciences, Harvard University, Cambridge, Massachusetts 02138, USA
[2]Department of Physics, Harvard University, Cambridge, Massachusetts 02138, USA
[3]HyperLight Corporation, 501 Massachusetts Ave, Cambridge, Massachusetts 02139, USA
*Corresponding author: loncar@seas.harvard.edu

Received 14 April 2020; revised 22 June 2020; accepted 28 July 2020 (Doc. ID 395114); published 8 September 2020

Crystals are ubiquitous in nature and are at the heart of material research, solid-state science, and quantum physics. Unfortunately, the controllability of solid-state crystals is limited by the complexity of many-body dynamics and the presence of defects. In contrast, synthetic crystal structures, realized by, e.g., optical lattices, have recently enabled the investigation of various physical processes in a controllable manner, and even the study of new phenomena. Past realizations of synthetic optical crystals were, however, limited in size and dimensionality. Here we theoretically propose and experimentally demonstrate optical frequency crystal of arbitrary dimensions, formed by hundreds of coupled spectral modes within an on-chip electro-optic frequency comb. We show a direct link between the measured optical transmission spectrum and the density of states of frequency crystals in one, two, three, and four dimensions, with no restrictions to further expanding the dimensionality. We demonstrate that the generation of classical electro-optic frequency comb can be modeled as a process described by random walks in a tight-binding model, and we have verified this by measuring the coherent distribution of optical steady states. We believe that our platform is a promising candidate for exploration of topological and quantum photonics in the frequency domain.

https://doi.org/10.1364/OPTICA.395114

1. INTRODUCTION

While nearly all solid-state crystal structures occurring in nature are three-dimensional, recent research efforts have resulted in the discoveries of lower-dimensional structures such as graphene or carbon nanotubes. Increasing the dimensionality of solid-state crystals is, however, implausible since they are bound by the three-dimensional Euclidian space. Extending the concept of high-dimensional spaces to crystal structures is an intriguing concept that has been studied from a theoretical standpoint [1,2]. In contrast to solid-state crystals, synthetic structures, realized by, e.g., optical lattices [3–11], have recently enabled the investigation of various physical processes in a controllable manner [4–9] and even the study of new phenomena [10,11]. High-dimensional synthetic crystal structures are of significant interest: they can be used to investigate complex dynamics of solid-state materials, where, e.g., the impact of forces, gauge fields, defects, or multi-particle interactions could be mapped to higher dimensions [12–14]. Furthermore, by mapping one system onto another with higher dimensionality, it becomes possible to solve certain problems more efficiently, which is the working principle of reservoir computers [15]. Synthetic crystals are also ideally suited to study complex dynamics in a highly controllable manner, since they are not restricted by physical space and can thus provide unique properties including high dimensionality. Optics, in particular, provides a powerful platform since the modes of light can be described by the same equations that govern the dynamics of many other physical systems. The realizations of synthetic optical structures have included measurements of classical and quantum correlations [4], Bloch oscillations [5], Anderson localization [6], Ising spin chains [7], quantum random walks [8], topological structures [9], as well as parity-time [10] and super-symmetric [11] lattices. Past realizations of synthetic photonic lattices were, however, limited in size and dimensionality, as they mainly relied on coupled optical waveguides or photonic crystals [5–11], i.e., a spatial degree of freedom on a two-dimensional plane. Recently, synthetic crystals have been theoretically proposed [12,13,16–19] and experimentally realized [20] employing the frequency domain of light.

Here we show that electro-optic frequency combs [21] can be modeled as a synthetic optical frequency crystal in high-dimensional space by means of a tight-binding model. In our approach, discrete lattice points are formed by spectral modes of an optical microring resonator realized in a thin-film lithium niobite (LN)-integrated photonic platform [22], while the coupling between lattice points is controlled by electro-optic phase modulation, enabled by the second-order nonlinearity of LN. Light coupled into the frequency crystals experiences coherent scattering and interference at different lattice points, in direct analogy to electron behavior in solid-state crystals. We show that it is possible to directly measure the density of states (DOS) of the frequency crystals with different dimensions and furthermore measure the signatures of coherent scattering processes on classical steady states such as Bloch oscillation and two-dimensional random walks.

2. FREQUENCY CRYSTALS AND DENSITY OF STATES

The tight-binding model is one of the most fundamental models in solid state physics [23] and is also extensively studied in optics: for example, it has been used to describe the physics of actively mode-locked lasers [24]. The tight-binding model assumes that particles (such as electrons or, here, photons) are localized at specific positions of the crystal lattice, and that they can hop between neighboring lattice points while preserving phase coherence. Optical tight-binding systems have in the past been realized using spatial modes in coupled optical waveguides [4–6,25] or temporal modes in coupled resonators with different round-trip times [10,26]. In contrast, here we experimentally realize synthetic crystal [13,16–19] utilizing the discrete frequency modes of a LN microring resonator [21]; see Fig. 1 and Supplement 1. By applying an electronic radio-frequency (RF) signal with a frequency equal to the separation between adjacent frequency modes (known as free spectral range, FSR), optical coupling can be initiated, where the coupling strength can be adjusted by the strength of the electric driving signal. Such an electro-optic resonator driven by a single-tone RF signal, commonly referred to as an electro-optical frequency comb source [21,27], can also be described in a one-dimensional tight-binding lattice [17] with a hopping rate related to the applied RF power. We here show that such a tight-binding frequency crystal representation is not limited to one-dimensional realizations. For example, using two RF signals (both only very slightly detuned from the resonator FSR), a photon placed in one optical resonance [Fig. 1(b)] can hop into neighboring resonances by the driving RF signal with a Hamiltonian described as

$$H = \sum_{j=-N}^{N} \left(\omega_j a_j^\dagger a_j + \sum_{i=1}^{d} \Omega_i \cos \omega_i t \left(a_j^\dagger a_{j+1} + \text{h.c.} \right) \right),$$

where a_j is the annihilation operator for mode j of the resonator with frequency ω_j, Ω_i is the coupling strength induced by the RF modulation, ω_i is the frequency of the RF signal, and d is the total number of RF signals ($d = 2$ in this example). Such a system can be described by a two-dimensional tight-binding model; see Supplement 1. Remarkably, we demonstrate that the same principle can be extended to three, four, and many more dimensions using different RF driving signals. Here each additional RF frequency tone can span an additional spectral dimension; see Fig. 1(b) and Supplement 1. Importantly, individual frequency modes within the microring resonators can be unambiguously mapped to individual lattice points within the crystal's synthetic frequency space; see Fig. 1. This high level of control and one-to-one mapping of spectral modes in real frequency space to lattice points in synthetic frequency space enables the experimental investigation of crystal structures in high dimensions.

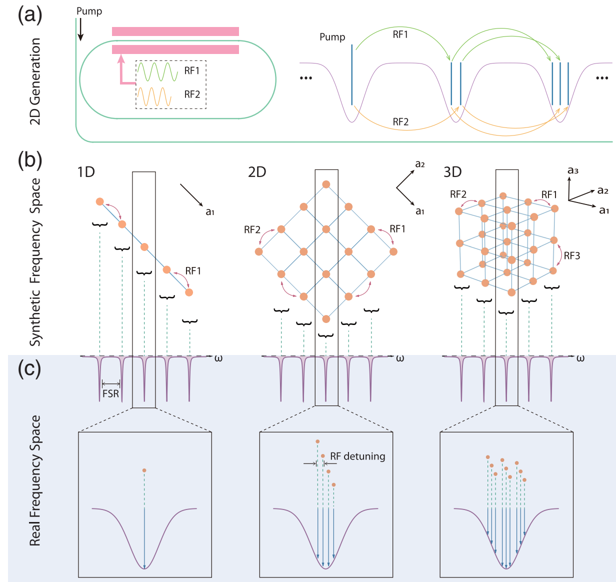

Fig. 1. Optical frequency crystals generation in electro-optic frequency comb source. (a) Schematic of the electro-optically modulated resonator used to generate the frequency crystals. The device consists of a waveguide-coupled race-track resonator with electrodes placed around it. The high-dimensional frequency crystals are formed by modulating the device with multiple, slightly detuned, RF signals (here two RF signals are shown for illustration). This gives rise to multiple excitations of each race-track resonance, each representing a crystal lattice point. (b) The tight-binding crystals can be represented in synthetic frequency space as fixed lattice points (yellow circle), where coupling between neighboring lattice points is mediated by electro-optic modulation due to the applied RF field. By modulating simultaneously with different frequencies, high-dimensional lattices can be generated in synthetic frequency space. (c) As a result, each optical resonance (mode of a resonator) represents one lattice point, one crystallographic direction, or one crystal plane of the synthetic frequency crystal when one, two, or three RF tones are applied, respectively. Within each resonance, the spacing between optical excitations is determined by the frequency difference between the RF driving signals.

Implementing the tight-binding model to describe the electro-optic frequency comb formation, we show that the frequency crystal's DOS can be directly measured by probing the optical transmission spectrum of the resonator; see Supplement 1. Specifically, we use input-output theory of optical resonators to establish a direct relationship between the optical transmission $T(\Delta)$ and DOS $D(\Delta)$ of the frequency crystals of arbitrary dimension, which is given by

$$T(\Delta) = 1 - 2\pi \frac{\kappa_e}{N_t^d} D(\Delta),$$

where Δ is wavelength detuning from the resonance center, κ_e is the external coupling rate of the resonator, d is the number of RF tones, and N_t is the total number of cavity resonance modes coupled by one RF tone ($\hbar$ is set to 1). The expression can be understood by considering that the larger DOS at given optical detuning corresponds to the larger the number of optical modes' excitation in reciprocal space of the frequency crystal. This leads to a larger effective optical "absorption" within the resonator, and thus smaller transmission; see Supplement 1. These results show that measuring the transmission spectrum of cavity resonance, using a tunable continuous-wave (CW) laser at telecom wavelengths,

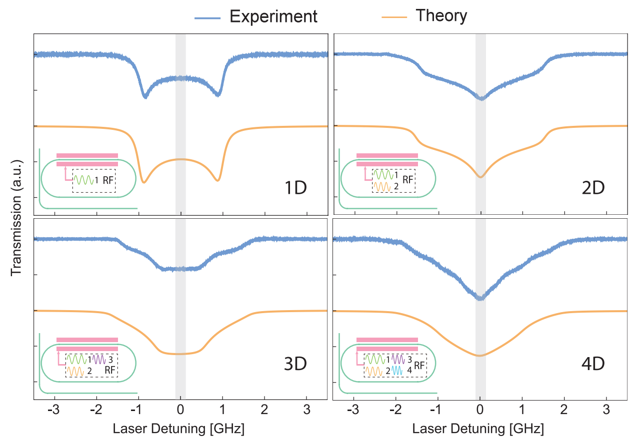

Fig. 2. DOS of high-dimensional frequency crystals. By scanning an excitation laser through the optical resonances, it becomes possible to directly measure the DOS of the frequency crystals. Shown is the measured normalized optical transmission (blue trace) for one- to four-dimensional crystals, superimposed with the analytical model (orange trace) based on the DOS of the frequency crystal. The grey shades represent the linewidth of the unmodulated resonance. a.u., arbitrary unit.

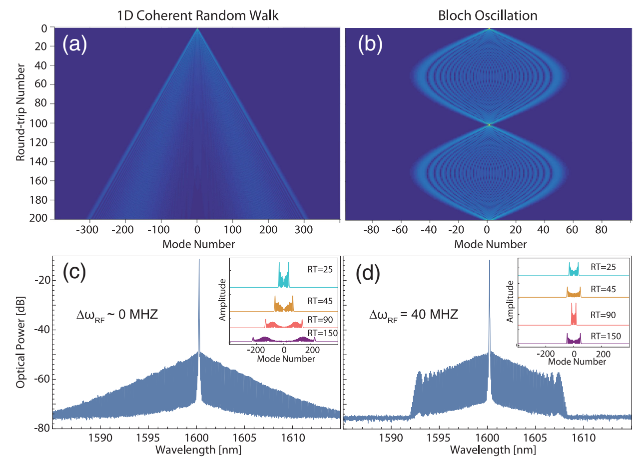

Fig. 3. Random walks and Bloch oscillations in one-dimensional frequency crystals. (a) In the absence of RF fields, CW laser excitation of the ring resonator leads to the excitation of one spectral mode (mode number 0), which is equivalent to the excitation of a single lattice point of a synthetic crystal. With RF fields are applied, photons can hop to neighboring optical modes, giving rise to a random walk and spectral broadening. Numerical simulations show that spectral modes with increasing mode number can be excited as light completes more round-trips (RTs) inside the resonator. Here the frequency of the RF drive was perfectly matched to the FSR of the resonator. (b) If the RF driving signal is detuned form the resonator FSR, an effective linear force is imposed, which leads to Bloch oscillations in the frequency domain. (c) In experiment, when the frequency crystal is excited with photons that are spectrally narrow enough to excite only a single lattice point, their temporal duration has to be larger than multiple round-trips. In such narrowband excitation, all round-trips of the random walks coherently interfere over the coherence time of the photon, forming a steady-state output with characteristic exponentially decaying spectrum. (d) In the presence of Bloch oscillations, a sharp cutoff in the optical output spectrum is measured, which arises from the oscillations in the random walks. The insets in (c) and (d) show numerical simulations for different RTs to illustrate the effect arising from the coherent addition of multiple coherent random walk round-trips.

represents a direct measurement of the DOS of the frequency crystal. Leveraging this analogy, we experimentally probed the DOS of one-, two-, three-, and four-dimensional frequency crystals, using up to four RF drives, and we found the result to be in excellent agreement with theoretical predictions (see Fig. 2). Furthermore, the resonances of a modulated resonator significantly broaden due to the formation of band structures of tight-binding frequency crystal, supporting a large number of spectral modes, which would not be supported in a static resonator; see Fig. 2. Here the cavity resonances are extracted from the raw measured data by fitting and removing the background Fabry–Perot resonance generated by reflection from chip facets. The FSR of the cavity is 10.453 GHz, and four different RF signals with frequency close to the FSR but detuned by 1 MHz from each other are applied (see Supplement 1). We note that the DOS of one-dimensional frequency lattices has recently been experimentally investigated [20].

3. RANDOM WALKS IN FREQUENCY CRYSTALS

A particularly important feature described by a tight-binding model is the occurrence of coherent random walks, which arise from the phase-coherent step-wise propagation of particles in a lattice [28]. Coherent random walks are also known as quantum walks [29]. Quantum walks with noninteracting photons can be probed with classical light, as each photon within the input beam undergoes the quantum walk, interferes with itself, and there is no interaction between photons [4,14]. Exciting our frequency crystal with noninteracting photons that have a narrow spectral linewidth (i.e., driving a single lattice point of the crystal in synthetic space) is expected to give rise to coherent random walk dynamics in the frequency domain, resulting in spectral spreading for each round-trip in the resonator [Fig. 3(a)]. However, photons that are spectrally narrow enough to only excite a single resonance intrinsically have to have a temporal duration much longer than the round-trip time of the resonator. For this reason, a description using individual round-trips cannot adequately describe the dynamics. In experiment, instead of experiencing discrete steps, multiple steps of the coherent random walk coherently interfere over the coherence time of the photon, forming a steady-state output when pumped classically; see Fig. 3(c) and Supplement 1. The interpretation here shows another way to understand the process of electro-optic frequency comb generation [21] and provides a means to model electro-optical combs at the single-photon level in the future.

Bloch oscillations are another well-known effect in solid-state physics, which occur in the presence of a linear force in the crystal. Theoretical considerations of one-dimensional frequency crystals have predicted that a linear force can be induced if the RF driving field is detuned from the spectral separation of the microring resonator modes [17]. In particular, with an RF modulation frequency significantly detuned from the FSR, spectral modes are generated detuned from the center of the resonances, which in turn induces additional phase shift. This effect is analogous to a phase shift induced by a linear force in solid-state crystals that are responsible for Bloch oscillations [17,30]. In the frequency crystal, these Bloch oscillations result in the relocalization of the light at the input frequency after a certain number of round-trips; see the simulation in Fig. 3(b). When excited with spectrally narrow photons, multiple round-trips coherently interfere over the coherence time

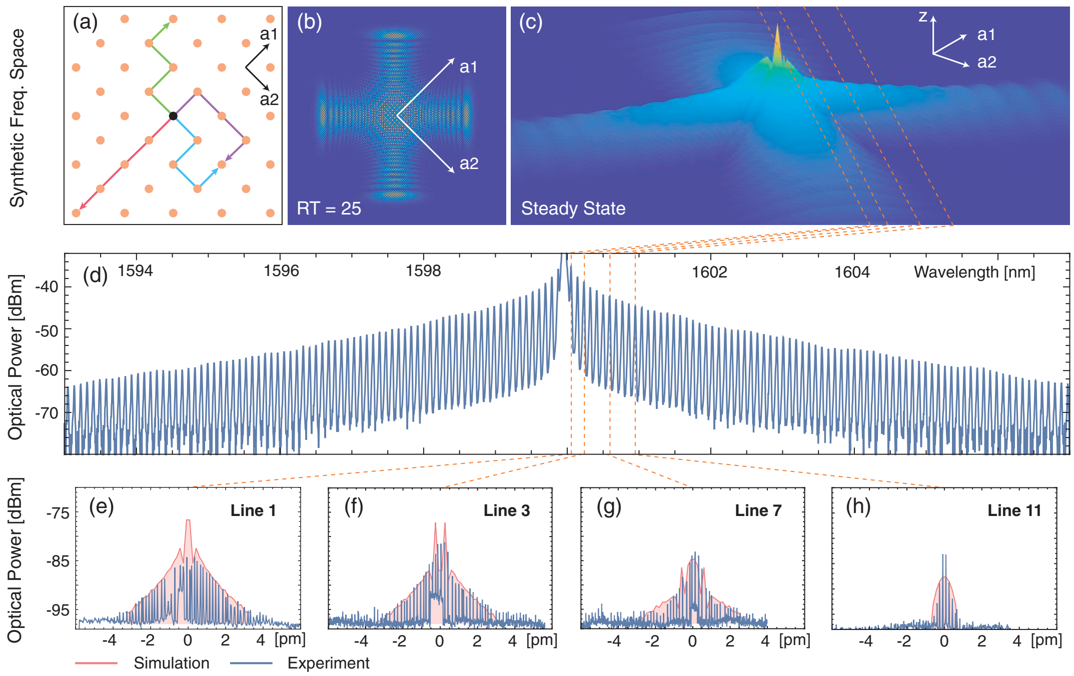

Fig. 4. Probing coherent random walks in two-dimensional synthetic crystals. (a). Illustration of possible paths that photon can take after four random walk steps (i.e., round-trips), if placed in the center of the 2D synthetic lattice. If the photon propagation is phase coherent, all possible paths leading to the same lattice point interfere, resulting in interference patterns in the probability distribution of the photon location in the lattice; see (b) for 25 simulated round-trips (RT). If the frequency crystal is excited with spectrally narrow photons (single lattice point excitation), multiple round-trips (RT = 1, 2, ..., N) coherently interfere, leading to a steady-state photon probability distribution in synthetic frequency space (the color and z axis represent the amplitude in logarithmic scale); see (c). The distribution in synthetic space can be mapped to measurable real frequency space; see Fig. 1. The emission spectrum in real frequency space was measured with an optical spectrum analyzer [(shown in (d)], while the spectral content within individual resonances was measured using heterodyne detection [shown in (e)–(h)]. As the spectral content within individual resonances is traced through the steady state in synthetic space, (e)–(f) broad spectra were expected and measured close to the excitation, while (g)–(h) narrow spectra were measured further away from the excitation.

of the photon, and the resulting steady-state solution shows a spectrum with interference fringes and clear cutoffs in the spectrum, which arises from the Bloch oscillations. In experiment with a CW pump, the cutoffs in the measured optical spectrum [Fig. 3(d)] agree with the simulations and represent a measured signature of Bloch oscillations in the frequency domain of light.

Considering two- and higher-dimensional frequency crystals, random walks are expected to appear in the synthetic frequency space [schematic in Fig. 1(b)], which maps into measurable signatures in real frequency space [schematic in Fig. 1(c)]. In a two-dimensional frequency crystal (formed by two RF modulation frequencies), photons positioned in a single lattice point can "hop" to one of the four nearest-neighbor lattice points per round-trip. Figure 4(a) shows examples of possible paths that a photon can take if placed at a single lattice point [e.g., at the center of Fig. 4(a)] within a 2D synthetic lattice. In classical, incoherent random walks, the different possible paths are independent, leading to a Gaussian probability distribution. In contrast, in coherent random walks, all possible paths are phase coherent and interfere, leading to a non-Gaussian probability distribution. We numerically simulated the probability distribution of a photon propagating in a frequency crystal, finding clear signatures of two-dimensional coherent random walks; see Fig. 4(b) for the simulated photon distribution after 25 round-trips. If excited with spectrally narrow photons, multiple random-walk steps coherently interfere and lead to a steady-state photon distribution in synthetic frequency space; see Fig. 4(c). The simulations show that as a consequence of the two-dimensional random walk, many spectral modes are excited within resonances close to the excitation frequency, while only a few frequency modes are excited for resonances far away from the excitation. Importantly, the photon distribution in synthetic space can be mapped onto the measurable real frequency space [see Fig. 1(c)], where the spectral content within resonances of the microring resonator represent cross sections through the synthetic frequency space; see Figs. 4(c) and 4(d). Using a heterodyne detection technique, we measure the spectral content of the resonances close to and far away from the excitation one; see Figs. 4(e)–4(h). As predicted theoretically, cavity resonances close to the excitation frequency contain many spectral modes [see Figs. 4(e) and 4(f)], while cavity resonances further away from the excitation contain significantly fewer lines (see Figs. 4(g) and 4(h)]. Thus, our measurements are consistent with predictions from the tight-binding model and two-dimensional coherent walks. Importantly, the observed spectral localization is relevant for the generation of broad electro-optic combs. Indeed, it has been shown that the spectral extent of electro-optic combs is mainly limited by a cutoff imposed by detuning of spectral modes from them center of the cavity resonances [21]. The observed random walks in frequency crystals might counter spectral cutoffs in the two-dimensional case. In particular, the process forces the photons to propagate mainly within the center of the resonances, where it experiences smaller resonator-induced phase shifts (i.e., linear forces) and therefore could enable broad comb generation when driven with multiple RF tones.

4. CONCLUSION AND OUTLOOK

In conclusion, we have theoretically proposed and experimentally demonstrated high-dimensional synthetic frequency crystals by driving an electro-optic resonator with multiple RF signals. Optical transmission measurements are demonstrated to be a powerful tool for the direct characterization of the DOS of frequency crystals. Theoretical simulation was applied to predict the signatures of Bloch oscillations and coherent random walks in frequency crystal. These results were also confirmed by our measurements in one- and two-dimensional frequency crystals. Furthermore, we performed, to the best of our knowledge, the first experimental characterizations of tight-binding systems with dimensionality larger than three. Our measurements were performed using spectrally narrow input light. In the future also excitation with light spectrally broader than the separation of synthetic lattice points can be investigated, which would correspond to exciting the synthetic crystal not in a single lattice point but in a superposition of points. Additionally, more complex RF signals can be implemented to change the lattice structure of the crystals. For example, it has been theoretically proposed that complex synthetic structures with nontrivial topologies could be generated by using multiple coupled and modulated resonators [23]. Our work also provides fundamental insight into the nature of electro-optical frequency comb formation, especially when driven with multiple RF signals. Finally, even though we used only classical light for the experimental realization, the measured features show clear signatures of quantum walks of noninteracting photons, which opens the door for future investigations using excitation with quantum light. In particular, we expect that our platform will enable new opportunities in frequency-domain quantum information processing [31,32] by exciting frequency crystals with, e.g., squeezed [33] or frequency-entangled [34] optical quantum states.

Funding. Air Force Office of Scientific Research (FA9550-19-1-0310); Office of Naval Research (QOMAND N00014-15-1-2761); National Science Foundation (EECS-1541959, DMR-1231319, ECCS- 1740296 E2CDA, ECCS-1609549).

Acknowledgment. We thank J. MacArthur for providing an RF source for the experiments, Cheng Wang and Shunyu Yao for helpful discussions, and B. Machielse and S. Bogdanovic for feedback on the manuscript.

Disclosures. The authors declare competing interests: C.R., M.Z., and M.L. are involved in developing lithium niobate technologies at HyperLight Corporation.

See Supplement 1 for supporting content.

†These authors contributed equally to this work.

REFERENCES

1. M. Skoge, A. Donev, F. H. Stillinger, and S. Torquato, "Packing hyperspheres in high-dimensional Euclidean spaces," Phys. Rev. E **74**, 041127 (2006).
2. C. E. Zachary and S. Torquato, "High-dimensional generalizations of the kagomé and diamond crystals and the decorrelation principle for periodic sphere packings," J. Stat. Mech. Theory Exp. **2011**, P10017 (2011).
3. L. Yuan, Q. Lin, M. Xiao, and S. Fan, "Synthetic dimension in photonics," Optica **5**, 1396–1405 (2018).
4. Y. Bromberg, Y. Lahini, R. Morandotti, and Y. Silberberg, "Quantum and classical correlations in waveguide lattices," Phys. Rev. Lett. **102**, 253904 (2009).
5. R. Morandotti, U. Peschel, J. S. Aitchison, H. S. Eisenberg, and Y. Silberberg, "Experimental observation of linear and nonlinear optical Bloch oscillations," Phys. Rev. Lett. **83**, 4756–4759 (1999).
6. Y. Lahini, A. Avidan, F. Pozzi, M. Sorel, R. Morandotti, D. N. Christodoulides, and Y. Silberberg, "Anderson localization and nonlinearity in one-dimensional disordered photonic lattices," Phys. Rev. Lett. **100**, 013906 (2008).
7. P. L. Mcmahon, P. L. Mcmahon, A. Marandi, Y. Haribara, R. Hamerly, C. Langrock, S. Tamate, T. Inagaki, H. Takesue, S. Utsunomiya, K. Aihara, R. L. Byer, M. M. Fejer, H. Mabuchi, and Y. Yamamoto, "A fully-programmable 100-spin coherent Ising machine with all-to-all connections," Science **354**, 614–617 (2016).
8. A. Peruzzo, M. Lobino, J. C. F. Matthews, N. Matsuda, A. Politi, K. Poulios, X.-Q. Zhou, Y. Lahini, N. Ismail, K. Wörhoff, Y. Bromberg, Y. Silberberg, M. G. Thompson, and J. L. OBrien, "Quantum walks of correlated particles," Science **329**, 1500–1503 (2010).
9. L. Lu, J. D. Joannopoulos, and M. Soljačić, "Topological photonics," Nat. Photonics **8**, 821–829 (2014).
10. A. Regensburger, C. Bersch, M. A. Miri, G. Onishchukov, D. N. Christodoulides, and U. Peschel, "Parity-time synthetic photonic lattices," Nature **488**, 167–171 (2012).
11. M. A. Miri, M. Heinrich, R. El-Ganainy, and D. N. Christodoulides, "Supersymmetric optical structures," Phys. Rev. Lett. **110**, 233902 (2013).
12. A. Celi, P. Massignan, J. Ruseckas, N. Goldman, I. B. Spielman, G. Juzeliunas, and M. Lewenstein, "Synthetic gauge fields in synthetic dimensions," Phys. Rev. Lett. **112**, 043001 (2014).
13. L. Yuan, Y. Shi, and S. Fan, "Photonic gauge potential in a system with a synthetic frequency dimension," Opt. Lett. **41**, 741–744 (2016).
14. A. Schreiber, A. Gábris, P. P. Rohde, K. Laiho, M. Stefanak, V. Potocek, C. Hamilton, I. Jex, and C. Silberhorn, "A 2D quantum walk simulation of two-particle dynamics," Science **336**, 55 (2012).
15. F. Duport, A. Smerieri, A. Akrout, M. Haelterman, and S. Massar, "Fully analogue photonic reservoir computer," Sci. Rep. **6**, 22381 (2016).
16. A. Schwartz and B. Fischer, "Laser mode hyper-combs," Opt. Express **21**, 6196–6204 (2013).
17. L. Yuan and S. Fan, "Bloch oscillation and unidirectional translation of frequency in a dynamically modulated ring resonator," Optica **3**, 1014–1018 (2016).
18. L. Yuan, M. Xiao, Q. Lin, and S. Fan, "Synthetic space with arbitrary dimensions in a few rings undergoing dynamic modulation," Phys. Rev. B **97**, 104105 (2018).
19. Q. Lin, M. Xiao, L. Yuan, and S. Fan, "Photonic Weyl point in a two-dimensional resonator lattice with a synthetic frequency dimension," Nat. Commun. **7**, 13731 (2016).
20. A. Dutt, M. Minkov, Q. Lin, L. Yuan, D. A. B. Miller, and S. Fan, "Experimental band structure spectroscopy along a synthetic dimension," Nat. Commun. **10**, 3122 (2019).
21. M. Zhang, B. Buscaino, C. Wang, A. Shams-Ansari, C. Reimer, R. Zhu, J. Kahn, and M. Loncar, "Broadband electro-optic frequency comb generation in a lithium niobate microring resonator," Nature **568**, 373–377 (2019).
22. M. Zhang, C. Wang, R. Cheng, A. Shams-Ansari, and M. Loncar, "Monolithic ultrahigh-Q lithium niobate microring resonator," Optica **4**, 1536–1537 (2017).
23. J. C. Slater and G. F. Koster, "Simplified LCAO method for the periodic potential problem," Phys. Rev. **94**, 1498–1524 (1954).
24. A. E. Siegman, *Lasers* (University Science Books, 1986).
25. P. Lai, X. Xu, Y. Wang, L. Qiao, A. Yang, and X. Jin, "Experimental two-dimensional quantum walk on a photonic chip," Sci. Adv. **4**, eaat3174 (2018).
26. A. Schreiber, K. N. Cassemiro, V. Potoček, A. Gábris, P. J. Mosley, E. Andersson, I. Jex, and C. Silberhorn, "Photons walking the line: a quantum walk with adjustable coin operations," Phys. Rev. Lett. **104**, 050502 (2010).
27. M. Kourogi, K. Nakagawa, and M. Ohtsu, "Wide-span optical frequency comb generator for accurate optical frequency difference measurement," IEEE J. Quantum Electron. **29**, 2693–2701 (1993).

28. H. Schmitz, R. Matjeschk, C. Schneider, J. Glueckert, M. Enderlein, T. Huber, and T. Schaetz, “Quantum walk of a trapped ion in phase space,” Phys. Rev. Lett. **103**, 090504 (2009).
29. S. E. Venegas-Andraca, “Quantum walks: a comprehensive review,” Quantum Inf. Process. **11**, 1015–1106 (2012).
30. N. R. A. Lee, M. Pechal, E. A. Wollack, P. Arrangoiz-Arriola, Z. Wang, and A. H. Safavi-Naeini, “Propagation of microwave photons along a synthetic dimension,” Phys. Rev. A **101**, 053807 (2020).
31. J. M. Lukens and P. Lougovski, “Frequency-encoded photonic qubits for scalable quantum information processing,” Optica **4**, 8–16 (2017).
32. H.-H. Lu, J. M. Lukens, N. A. Peters, B. P. Williams, A. M. Weiner, and P. Lougovski, “Quantum interference and correlation control of frequency-bin qubits,” Optica **5**, 1455 (2018).
33. J. Roslund, R. M. de Araújo, S. Jiang, C. Fabre, and N. Treps, “Wavelength-multiplexed quantum networks with ultrafast frequency combs,” Nat. Photonics **8**, 109–112 (2013).
34. M. Kues, C. Reimer, P. Roztocki, L. R. Cortés, S. Sciara, B. Wetzel, Y. Zhang, A. Cino, S. T. Chu, B. E. Little, D. J. Moss, L. Caspani, J. Azaña, and R. Morandotti, “On-chip generation of high-dimensional entangled quantum states and their coherent control,” Nature **546**, 622–626 (2017).